

# Modeling of an MHD Free Surface Problem Arising in CZ Crystal Growth

R. Griesse, Johann Radon Institute for Computational and Applied Mathematics, Linz, Austria  
 A. J. Meir, Department of Mathematics and Statistics, Auburn University, USA

Corresponding Author: R. Griesse  
 Johann Radon Institute for Computational and Applied Mathematics  
 Austrian Academy of Sciences  
 Altenbergerstraße 69, 4040 Linz, Austria  
 e-mail: roland.griesse@oeaw.ac.at

**Abstract.** A free surface problem arising in the Czochralski (CZ) crystal growth process is considered. A mathematical model accounting for the interaction of the molten material with applied and induced magnetic fields, temperature-induced convection, rotating boundaries and a free surface is given. The model described avoids some common simplifying assumptions and allows for more general geometries, and non axisymmetric (fully three-dimensional) flow fields. It accounts for the induced magnetic field and avoids nonrealistic idealized boundary conditions on the magnetic field.

**Keywords.** Magnetohydrodynamics, mathematical modeling, free surface, crystal growth, Czochralski process

## 1. Introduction

In this paper we consider some aspects concerning the mathematical modeling of free surface problems arising in technical processes which involve the interaction of electrically conducting fluids and magnetic fields, described by the equations of magnetohydrodynamics (MHD). To focus the discussion, we restrict ourselves to the Czochralski (CZ) process in crystal growth. However, our model can readily be extended to, e.g., continuous casting problems which are described in [1, 3, 18, 19], and the references therein, and to aluminum reduction cells, see, e.g., [2, 5, 7].

The CZ crystal growth process is used, for instance, to grow silicon crystals for the semiconductor industry. The silicon is melted inside a crucible before a seed is lowered into the melt to initiate the crystallization process. The seed is slowly pulled upwards, and the pulling speed determines the diameter of the ingot. A schematic of the CZ process is shown in Figure 1. For a review paper describing this process, we refer to [16].

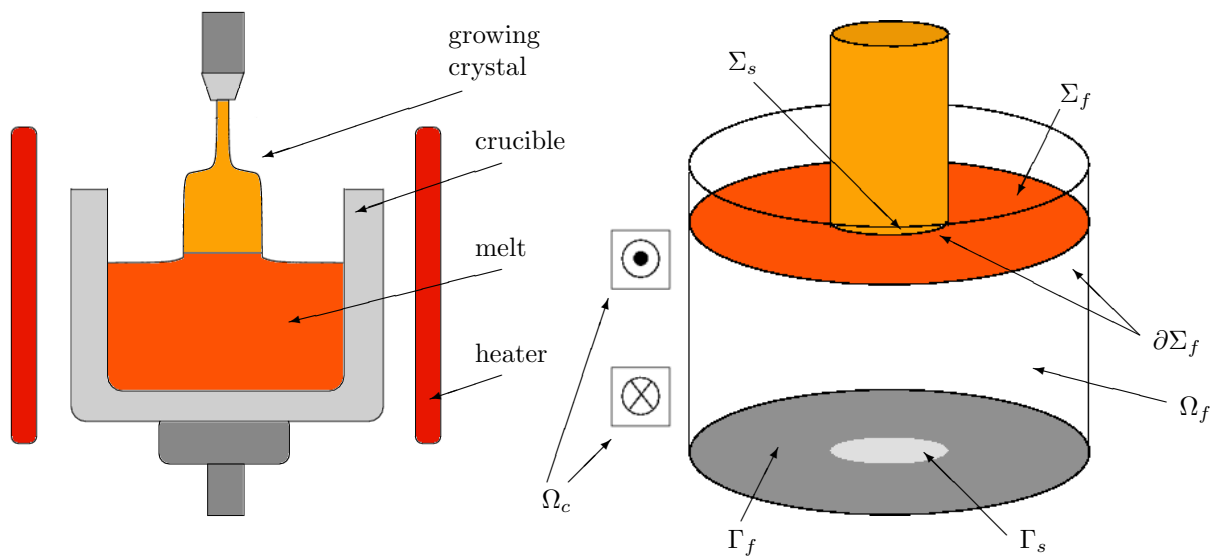


Figure 1: Schematic of the CZ process and geometry of the free surface problem.

Due to temperature gradients in the hot melt, a strong buoyancy-driven flow can develop. In the presence of a free surface, surface tension and its variation with temperature also drives fluid motion, known as the Marangoni effect. In addition, both the seed and the crucible are often rotated. Rotating or steady magnetic fields may be applied to influence the fluid motion in a favorable way. Some of the concerns are non-uniform dopant distribution and impurity striations. The goals include the reduction of radial and axial temperature gradients and a flow field close to an axisymmetric configuration, in order to homogenize solute concentration. In addition, it is desired to damp out flow instabilities, or to overpower turbulence which otherwise lead to deterioration of the final crystal's properties, see, e.g., [9, 10, 20–22, 24–26].

The current work differs from prior work in a number of aspects. One main feature of the model presented is the use of the electric current density rather than the magnetic field as the primary electromagnetic variable. This is known as the velocity-current formulation of the MHD equations (see [13] and [14]). Here the induced magnetic field is recovered from the current density via the Biot-Savart law making idealized or artificial electromagnetic boundary conditions unnecessary. This allows us to account for the interior and exterior magnetic fields even though the equations are posed on the (bounded) fluid and conductor regions. It also allows for coupling between the conducting fluid and external conductors (the electromagnetic principle of *action at a distance*).

In addition, we do not assume that the equations decouple or partially decouple, allowing for separation of fluid field, electromagnetic field, and temperature field computations. Earlier work had been mostly restricted to situations without such coupling and required some unrealistic simplifying assumptions, e.g., small magnetic Reynolds number, and vessels with perfectly conducting or insulating walls. Moreover, we do not neglect the induced magnetic fields, the electromagnetic interaction of the melt with other conductors in its vicinity, or buoyancy due to temperature fluctuations.

In contrast to most prior work we do not assume that the flow is two-dimensional and allow for fully three-dimensional flows. Note that even in the very simple situation of a rotating cylinder, the flow is fully three-dimensional in the presence of a transverse magnetic field (see [15]). Hence we describe a fully coupled three-dimensional model allowing the full system of hydrodynamic and electromagnetic equations under realistic interface conditions for the magnetic field.

## 2. Mathematical Modeling

As the growth of an actual crystal in practice is a tremendously complicated process, we focus here only on some of the aspects, for which we give a mathematical model. In particular, we include the interaction of the conducting melt with magnetic fields, the temperature-induced convection, the free surface, and the rotation of the solidified crystal and the crucible. To emphasize these ideas we do not pay attention to the detailed modeling of heat sources to maintain the melt temperature, and neither to the interaction of the magnetic fields with the crucible, the heater, and other components of an actual crystal growing device. However, it is straightforward to generalize the model to account for these. In addition, since the growth proceeds slowly and we consider only a small time interval, we give all equations in their stationary form. This implies that we also neglect the pull velocity which is usually much smaller than the rotational velocity of the crucible or fluid velocity in the melt. An extension that takes into account instationary phenomena is of course possible.

As shown in Figure 1, the electrically conducting fluid occupies a bounded domain  $\Omega_f \subset \mathbb{R}^3$ . We further assume that the fluid may be under the influence of applied magnetic fields, some of which may be the result of electric currents flowing in various conductors  $\Omega_c \subset \mathbb{R}^3$ . Thus the region of space we include in this model is  $\Omega = \Omega_f \cup \Omega_c \subset \mathbb{R}^3$ , a bounded domain which contains the fluid domain and the various electrically conducting regions which we account for.

We further assume that the fluid partially fills a container, and the fluid region is in part bounded above by the solid crystal (the solidification front is denoted by  $\Sigma_s$ ) and in part by a free surface  $\Sigma_f$ . The surface  $\Sigma_f$  is not prescribed and so we are dealing with a free boundary (free surface) problem. For a brief introduction to capillary surfaces see [6] and the references therein. In the configuration depicted in Figure 1, the container is cylindrical in shape. We denote by  $\Gamma = \Gamma_f \cup \Gamma_s$  the base of the container, where  $\Gamma_s$  is the projection of  $\Sigma_s$  onto the container's base and  $\Gamma_f$  is the projection of the free surface onto the container's base. Both are open sets in  $\mathbb{R}^2$ .

## 2.1 The Equations for a Fixed Fluid Domain

To set the stage we begin by considering the MHD equations on a fixed domain (where the fluid completely fills the container and there is no free surface). The equations, in the fluid region  $\Omega_f$ , are the MHD equations, that is the Navier Stokes equations coupled to the quasi-stationary form of Maxwell's equations via Ohm's law (and the Lorentz force)

$$\begin{aligned} -\eta\Delta\mathbf{u} + \rho(\mathbf{u} \cdot \nabla)\mathbf{u} + \nabla p - \mathbf{J} \times \mathbf{B} &= \mathbf{F} \\ \nabla \cdot \mathbf{u} &= 0. \end{aligned}$$

Here  $\mathbf{u}$  is the fluid velocity,  $p$  the pressure,  $\mathbf{J}$  electric current density,  $\mathbf{B}$  magnetic field (actually magnetic induction),  $\mathbf{F}$  a body force (addressed later),  $\eta$  the fluid's viscosity, and  $\rho$  the fluid's density.

Maxwell's equations hold on all of  $\mathbb{R}^3$

$$\nabla \times (\mu^{-1}\mathbf{B}) = \mathbf{J} \quad \nabla \cdot \mathbf{B} = 0 \quad (1)$$

$$\nabla \times \mathbf{E} = 0 \quad \nabla \cdot \mathbf{E} = 0, \quad (2)$$

where the charge density is neglected as is usual in the MHD approximation. Here  $\mu$  is the magnetic permeability and  $\mathbf{E}$  the electric field.

Ohm's law takes on various forms in the various sub-domains under consideration

$$\mathbf{J} = \begin{cases} \sigma(\mathbf{E} + \mathbf{u} \times \mathbf{B}) & \text{in } \Omega_f, \text{ the fluid region} \\ \sigma\mathbf{E} + \mathbf{J}_0 & \text{in } \Omega_c, \text{ external conductors} \\ 0 & \text{elsewhere.} \end{cases} \quad (3)$$

Here  $\sigma$  is the electrical conductivity of the fluid or the external conductors, respectively, and  $\mathbf{J}_0$  is a prescribed electric current density. The current in external conductors  $\Omega_c$  is usually driven by a current or voltage source. If this is included in the model, the current density in the external conductors becomes an additional unknown satisfying  $\mathbf{J} = \sigma\mathbf{E}$  in  $\Omega_c$ . However, we consider  $\mathbf{J}_0$  to be given here. Compatible boundary conditions for the above equations are

$$\mathbf{u}|_{\partial\Omega_f} = \mathbf{u}_0 \quad \text{with} \quad \int_{\partial\Omega_f} \mathbf{u}_0 \cdot \mathbf{n} = 0. \quad (4)$$

Throughout,  $\mathbf{n}$  will denote an outward pointing unit vector normal to the fluid domain  $\Omega_f$ . Boundary condition (4) allows for rotation of the crucible. Other boundary conditions involving the stress, or a combination of stress components and velocity components may be prescribed and are needed to include the free surface into our model, see Section 2.2 (general boundary conditions that result in well posed problems were formulated and studied in [4]). As boundary conditions for the current we have

$$\begin{aligned} \mathbf{J} \cdot \mathbf{n}|_{\partial\Omega_f} &= 0 \\ \mathbf{J} \cdot \mathbf{n}|_{\partial\Omega_c} &= 0. \end{aligned} \quad (5)$$

In the second equation,  $\mathbf{n}$  exceptionally denotes an outward normal to  $\Omega_c$ . That is, the fluid container and the external conductors are insulated and there is no current flow through their boundaries. In case some of the external conductors are attached to the fluid region  $\Omega_f$ , these boundary conditions must be changed to ensure continuity of the current across the attached areas, see, e.g., [4, 14, 15].

The electric field and magnetic field must satisfy the following interface conditions:

$$\begin{aligned} [\mathbf{B} \cdot \mathbf{n}]_{\partial\Omega_f} &= 0 & [\mathbf{E}]_{\partial\Omega_f} &= 0 \\ [\mu^{-1}\mathbf{B} \times \mathbf{n}]_{\partial\Omega_f} &= -\mathbf{J}_{\partial\Omega_f} \end{aligned}$$

where  $[\cdot]_s$  denotes the jump across the surface  $s$ , and  $\mathbf{J}_{\partial\Omega_f}$  is a given surface current. The surface current  $\mathbf{J}_{\partial\Omega_f}$  can be assumed zero. This is evident if the fluid container is an electrical insulator. Otherwise, if it has finite thickness, we can treat it as an additional conductor, solve Ohm's law (3) there as well, and alter the boundary conditions (5) to reflect continuity of the current across the fluid/container interface.

Moreover, we have radiation conditions at infinity

$$\mathbf{B} = \mathbf{B}_\infty \quad \mathbf{E} = \mathbf{E}_\infty .$$

In order to simplify numerical simulations for the above system, avoid having to explicitly solve Maxwell's equations on all of space, and reduce the computations so that only unknowns defined on a the bounded domain  $\Omega$  are involved one can employ the, so-called, velocity-current formulation, see [14]. This formulation takes into account the fact that the magnetic field  $\mathbf{B}$  is induced by the current  $\mathbf{J}$  in the fluid and in the external conductors, see (1). This induced field can be obtained by employing the Biot-Savart law,

$$\mathbf{B}(\mathbf{x}) = \mathcal{B}(\mathbf{J})(\mathbf{x}) = -\frac{\mu}{4\pi} \int_{\mathbb{R}^3} \frac{\mathbf{x} - \mathbf{y}}{|\mathbf{x} - \mathbf{y}|^3} \times \mathbf{J}(\mathbf{y}) d^3 \mathbf{y} .$$

Note that since the current vanishes outside the conductors, the integral actually extends only over the bounded set  $\Omega_f \cup \Omega_c$ . The Biot-Savart operator ensures that

$$\begin{aligned} \nabla \times \mathbf{B} &= \mu \mathbf{J}, & \nabla \cdot \mathbf{B} &= 0 \quad \text{on } \mathbb{R}^3 \\ [\mathbf{B}]_{\partial\Omega_f} &= 0 & \mathbf{B} &= 0 \quad \text{at infinity.} \end{aligned}$$

Moreover, we may substitute the curl-free electric field  $\mathbf{E}$  by its potential,

$$\mathbf{E} = -\nabla\phi .$$

Now the equations, in the fluid region  $\Omega_f$  are

$$-\eta\Delta\mathbf{u} + \rho(\mathbf{u} \cdot \nabla)\mathbf{u} + \nabla p - \mathbf{J} \times \mathcal{B}(\mathbf{J}) = \mathbf{F} \quad \nabla \cdot \mathbf{u} = 0 \quad (6)$$

$$\sigma^{-1}\mathbf{J} + \nabla\phi - \mathbf{u} \times \mathcal{B}(\mathbf{J}) = 0 \quad \nabla \cdot \mathbf{J} = 0. \quad (7)$$

In case an additional applied magnetic field  $\mathbf{B}_0$  is present, such as a field generated by a permanent magnet, we replace  $\mathcal{B}(\mathbf{J})$  by  $\mathcal{B}(\mathbf{J}) + \mathbf{B}_0$ .

In order to model convection-driven flow, we also add an equation for the temperature (energy equation) and couple it to the momentum equation using the Boussinesq approximation. That is, the density dependence on the temperature is neglected except in the buoyancy term. The right hand side of the momentum equation becomes

$$\mathbf{F} = \rho [1 - \beta(T - T_{\text{ref}})] \mathbf{g} .$$

Here  $T_{\text{ref}}$  is a reference temperature,  $\beta$  is the thermal expansion coefficient, and  $\mathbf{g}$  is the acceleration of gravity.

The energy equation is

$$-\kappa\Delta T + \rho c_p (\mathbf{u} \cdot \nabla) T = Q \quad \text{in } \Omega_f, \quad (8)$$

where  $\kappa$  is the fluid's thermal conductivity,  $c_p$  is its specific heat at constant pressure, and  $Q$  is some heat source. The heat source can be

$$Q = \sigma^{-1} |\mathbf{J}|^2 + \frac{1}{2} \eta |\nabla\mathbf{u} + (\nabla\mathbf{u})^\top|^2 + q$$

where the first term on the right is due to Joule dissipation, the second due to viscous heating, and the third can account for additional heat sources. In many situations, the first and second term in  $Q$  are negligibly small, see, e.g., [17].

The boundary condition for the temperature can of course be of Dirichlet type (prescribed temperature), Neumann type (prescribed heat flux through the boundary), or (mixed) Robin type representing Newton's law of cooling

$$-\kappa(\nabla T) \cdot \mathbf{n} = \alpha(T - T_{\text{ext}}) \quad \text{on } \partial\Omega_f. \quad (9a)$$

The latter is a linearization of Boltzmann's law of radiation

$$-\kappa(\nabla T) \cdot \mathbf{n} = \sigma_B \varepsilon (T^4 - T_{\text{ext}}^4) \quad \text{on } \partial\Omega_f \quad (9b)$$

with Boltzmann constant  $\sigma_B$  and surface emissivity  $\varepsilon$ , which will be more appropriate when the relevant temperature range is large.

For convenience, we write

$$T = \Theta(\mathbf{u}, \mathbf{J})$$

where  $\Theta$  is the solution operator of the temperature equation (8) and boundary conditions (9), for a given velocity and current density. Thus we write  $\mathbf{F}$  as

$$\mathbf{F} = \rho [1 - \beta(\Theta(\mathbf{u}, \mathbf{J}) - T_{\text{ref}})] \mathbf{g}. \quad (10)$$

Now the equations, in the fluid region  $\Omega_f$  are

$$-\eta \Delta \mathbf{u} + \rho(\mathbf{u} \cdot \nabla) \mathbf{u} + \nabla p - \mathbf{J} \times \mathcal{B}(\mathbf{J}) = \rho [1 - \beta(\Theta(\mathbf{u}, \mathbf{J}) - T_{\text{ref}})] \mathbf{g} \quad \nabla \cdot \mathbf{u} = 0 \quad (11)$$

$$\sigma^{-1} \mathbf{J} + \nabla \phi - \mathbf{u} \times \mathcal{B}(\mathbf{J}) = 0 \quad \nabla \cdot \mathbf{J} = 0, \quad (12)$$

which must be complemented by appropriate boundary conditions for the velocity (4), and the current (5). We emphasize that the various coefficients in our equations may be temperature-dependent. In particular, this applies to the conductivity  $\sigma$  and thermal conductivity  $\kappa$ . We also remind the reader that  $\mathcal{B}$  and  $\Theta$  are integral operators (defined above).

## 2.2 The Free Boundary Value Problem

We now consider the free boundary value problem where part of the fluid's top surface  $\Sigma_f$  is not prescribed, see [6] and the references therein. To be precise, the free surface extends from the lateral container walls inward to the solidified ingot, see Figure 1. For simplicity we assume that the crystal-melt interface  $\Sigma_s$  is known. Of course more generally one can find the position and shape of this interface by also solving the heat equation in the crystal and employing a Stefan-type condition at this interface.

For the free surface problem, we modify the previously given boundary conditions, e.g., (9a) or (9b) and impose

$$T = T_{\text{melt}} \quad \text{on } \Sigma_s \quad (13)$$

where the solidified crystal comes in contact with the melt, see Figure 1.  $T_{\text{melt}}$  is the melting temperature of the respective material. On the free surface and the rest of the fluid domain's boundary (that is on  $\partial\Omega_f \setminus \overline{\Sigma}_s$ ), the previously given boundary conditions apply, e.g., of Newton or Boltzmann radiation type.

We now address the characterization of the free surface and appropriate boundary conditions. Let us denote by  $\mathcal{T} = -pI + \eta(\nabla \mathbf{u} + (\nabla \mathbf{u})^\top)$  the total stress tensor of the fluid. We recall our equations on  $\Omega_f$

$$\begin{aligned} -\eta \nabla \cdot (\nabla \mathbf{u} + (\nabla \mathbf{u})^\top) + \rho(\mathbf{u} \cdot \nabla) \mathbf{u} + \nabla p - \mathbf{J} \times \mathcal{B}(\mathbf{J}) &= \rho [1 - \beta(\Theta(\mathbf{u}, \mathbf{J}) - T_{\text{ref}})] \mathbf{g} & \nabla \cdot \mathbf{u} &= 0 \\ \sigma^{-1} \mathbf{J} + \nabla \phi - \mathbf{u} \times \mathcal{B}(\mathbf{J}) &= 0 & \nabla \cdot \mathbf{J} &= 0, \end{aligned}$$

where for convenience we replaced the  $\Delta \mathbf{u}$  term in the momentum equation by  $\nabla \cdot (\nabla \mathbf{u} + (\nabla \mathbf{u})^\top)$  so that the conditions imposed on the stress below become natural boundary conditions.

As in Section 2.1, we impose the velocity boundary condition

$$\mathbf{u}|_{\partial\Omega_f \setminus \overline{\Sigma}_f} = \mathbf{u}_0 \quad (14)$$

at the crucible and crystal surfaces, where the given boundary velocity  $\mathbf{u}_0$  accounts for possible rotation of the crucible and the crystal ingot.

We describe the deviation from a flat surface (the fluid's top surface when at rest) as the graph of some function  $H$  which is defined on  $\Gamma_f$ , the projection of  $\Sigma_f$  onto the crucible's base  $\Gamma$ , see Figure 1. In order to determine  $H$  and to specify the fluid boundary conditions on the free surface, we need to provide four scalar equations. For free interfaces, conditions on the jump of the stress tensor across the interface are appropriate. Note that as the surrounding atmosphere is at rest, its total stress tensor is simply  $-p_{\text{atm}}I$  where  $p_{\text{atm}}$  is the atmospheric pressure.

The Laplace-Young equation states that the jump of the normal stresses across the interface is equal to the product of the surface tension coefficient  $\gamma$  and the curvature of the interface. Note that the surface curvature is given by

$$\nabla' \cdot \frac{\nabla' H}{\sqrt{1 + |\nabla' H|^2}},$$

where  $\nabla' \cdot (\cdot)$  and  $\nabla'(\cdot)$  are the surface divergence and gradient, respectively. This yields our first condition

$$-\gamma \nabla' \cdot \frac{\nabla' H}{\sqrt{1 + |\nabla' H|^2}} + p_{atm} = -(\mathcal{T} \cdot \mathbf{n}) \cdot \mathbf{n} = p - \eta ((\nabla \mathbf{u} + (\nabla \mathbf{u})^\top) \cdot \mathbf{n}) \cdot \mathbf{n} \quad \text{on } \Gamma_f. \quad (15)$$

Note that in the above equation, we abuse notation since the right hand side is to be evaluated on the free surface  $\Sigma_f$  rather than on its projection  $\Gamma_f$ . Equation (15) is a second-order partial differential equation which, together with the associated conditions (16)–(17), determines the location of the free surface. As a boundary condition for  $H$  we have

$$\nabla' H \cdot \mathbf{n}'|_{\partial \Gamma_f} = 0. \quad (16)$$

Here  $\partial \Gamma_f$  is the projection of  $\partial \Sigma_f$  onto  $\Gamma$  and  $\mathbf{n}'$  is the planar outward pointing unit normal vector to  $\Gamma_f$ . The curves  $\partial \Sigma_f$  are the so-called contact lines, i.e., the curves along which the fluid's free surface comes in contact with the container wall and the solid crystal, see Figure 1. Thus the condition (16) is a condition on the contact angle. Here we specify that the fluid attaches to the wall and the solidified crystal with a  $90^\circ$  angle, and of course other angles can be specified. The contact angle is a material property which may be affected by surface treatments, see [6]. We also have the constraint

$$\int_{\Gamma_f} H dx = 0 \quad (17)$$

which amounts to conservation of fluid volume. Note that here we continue to employ the underlying assumption from the Boussinesq approximation, that the density is constant except in the buoyancy term. In addition, we have assumed that the consumption of melt due to crystallization is negligible compared to the volume of the liquid pool.

The second and third conditions determine the jump of the tangential stresses across the free surface by equating it with the gradient of the surface tension  $\gamma$ . In our model, we account for variations in  $\gamma$  with temperature which give rise to the so-called Marangoni effect, which can be significant in crystal growth problems [11, 12]. We obtain

$$\mathcal{T} \cdot \mathbf{n} - ((\mathcal{T} \cdot \mathbf{n}) \cdot \mathbf{n}) \cdot \mathbf{n} = \frac{d\gamma}{dT} (\nabla \Theta(\mathbf{u}, \mathbf{J}) - (\nabla \Theta(\mathbf{u}, \mathbf{J}) \cdot \mathbf{n}) \mathbf{n}) \quad \text{on } \Sigma_f. \quad (18)$$

Note that (18) yields non-trivial conditions only in directions perpendicular to the surface normal  $\mathbf{n}$ . As the fourth and final condition, we impose the non-penetration constraint

$$\mathbf{u} \cdot \mathbf{n}|_{\Sigma_f} = 0. \quad (19)$$

### 3. Outlook

The free surface model described above can serve as the basis for numerical computations. Note that due to the velocity-current formulation, all unknown quantities are confined to the fluid domain  $\Omega_f$ . On the one hand, numerical simulations can improve the understanding of the complex phenomena and interactions in the Czochralski growth process, compare, e.g., [11, 12].

On the other hand, there is a strong interest in optimizing crystal growth processes with respect to time and product quality. To this end, one has a number of parameters at one's disposal. These include control of the heat sources, the location, strength and configuration of applied magnetic fields, and the rotation and pulling speeds, see, e.g., [9, 23]. In addition, suitable optimization criteria have to be defined. So far, the attempts at optimizing CZ and related processes seem to be based on indirect quality indicators, such as the deviation of the flow field from a desired one. This leads to objective functionals involving terms such as

$$\int_{\Omega_f} |\mathbf{u} - \mathbf{u}_d|^2 dx, \quad \int_{\Omega_f} |\nabla \times \mathbf{u}|^2 dx, \quad \text{and} \quad \int_{\Omega_f} |\nabla T|^2 dx.$$

Above, the first term represents the desire to steer the flow towards a desired flow field  $\mathbf{u}_d$ , for instance, the velocity field of rigid body rotation, compare [25]; the second term, the desire to reduce the vorticity; and the third term, the desire to reduce temperature gradients in the melt.

We also refer to [8] for a generic optimal control problem for the stationary MHD equations in velocity–current form. Certainly, another major challenge is use direct quality indicators such as dopant distribution as the basis for optimization. This, however, requires more advanced mathematical models.

#### 4. References

- [1] A. Bermúdez and M. C. Muñiz. Numerical solution of a free boundary problem taking place in electromagnetic casting. *Mathematical Models and Methods in Applied Sciences*, 9(9):1393–1416, 1999.
- [2] A. Bermúdez, M. C. Muñiz, and P. Quintela. Existence and uniqueness for a free boundary problem in aluminum electrolysis. *J. Math. Anal. Appl.*, 191(3):497–527, 1995.
- [3] O. Besson, J. Borgeois, P.-A. Chevalier, J. Rappaz, and R. Touzani. Numerical modeling of electromagnetic casting processes. *Journal of Computational Physics*, 92:482–507, 1991.
- [4] M. Charina, A. J. Meir, and P. G. Schmidt. Mixed velocity, stress, current, and potential boundary conditions for stationary MHD flow. *Computers Math. Appl.*, 48:1181–1190, 2004.
- [5] J. Descloux, M. Flueck, and M. V. Romerio. A modelling of the stability of aluminium electrolysis cells. In *Nonlinear partial differential equations and their applications. Collège de France Seminar, Vol. XIII (Paris, 1994/1996)*, volume 391 of *Pitman Res. Notes Math. Ser.*, pages 117–133. Longman, Harlow, 1998.
- [6] R. Finn. Capillary surface interfaces. *Notices of the AMS*, 46(7):770–781, 1999.
- [7] J.-F. Gerbeau, C. Le Bris, and T. Lelièvre. Simulations of MHD flows with moving interfaces. *Journal of Computational Physics*, 184(1):163–191, 2003.
- [8] R. Griesse and K. Kunisch. Optimal control for a stationary MHD system in velocity–current formulation. *submitted*, 2004. <http://www.ricam.oeaw.ac.at/people/page/griesse/publications.html>.
- [9] M. Gunzburger, E. Ozugurlu, J. Turner, and H. Zhang. Controlling transport phenomena in the czochralski crystal growth process. *Journal of Crystal Growth*, 234:47–62, 2002.
- [10] H. Hirata and K. Hoshikawa. Silicon crystal growth in a cusp magnetic field. *Journal of Crystal Growth*, 96:745–755, 1989.
- [11] V. Kumar, B. Basu, S. Enger, G. Brenner, and F. Durst. Role of Marangoni convection in Si-Czochralski melts—Part I: 3d predictions with crystal rotation. *Journal of Crystal Growth*, 255:27–39, 2003.
- [12] V. Kumar, B. Basu, S. Enger, G. Brenner, and F. Durst. Role of Marangoni convection in Si-Czochralski melts—Part II: 3d predictions without crystal. *Journal of Crystal Growth*, 253:142–154, 2003.
- [13] A. J. Meir and P. G. Schmidt. Variational methods for stationary MHD flow under natural interface conditions. *Nonlinear Anal.*, 26(4):659–689, 1996.
- [14] A. J. Meir and P. G. Schmidt. Analysis and numerical approximation of a stationary MHD flow problem with nonideal boundary. *SIAM J. Numer. Anal.*, 36(4):1304–1332, 1999.
- [15] A. J. Meir, P. G. Schmidt, S. I. Bhaktiyarov, and R. A. Overfelt. Numerical simulation of steady liquid-metal flow in the presence of a static magnetic field. *Trans. ASME J. Appl. Mech.*, 71(6):786–795, 2004.

- [16] V. Prasad, H. Zhang, and A. P. Anselmo. Transport phenomena in Czochralski crystal growth processes. In *Advances in heat transfer*, volume 30, pages 313–435. Academic Press, 1997.
- [17] P. Prescott and F. Incropera. Magnetically damped convection during solidification of a binary metal alloy. *Journal of Heat Transfer*, 115:302–309, 1993.
- [18] J. Rappaz and R. Touzani. On a two-dimensional magnetohydrodynamic problem I. modeling and analysis. *M2AN Mathematical Modeling and Numerical Analysis*, 26(2):347–364, 1991.
- [19] J. Rappaz and R. Touzani. On a two-dimensional magnetohydrodynamic problem II. numerical analysis. *M2AN Mathematical Modeling and Numerical Analysis*, 30(2):215–235, 1996.
- [20] R. W. Series. Effects of a shaped magnetic field in Czochralski silicon growth. *Journal of Crystal Growth*, 97:92–98, 1989.
- [21] R. W. Series and D. T. J. Hurle. The use of magnetic fields in semiconductor crystal growth. *Journal of Crystal Growth*, 113:305–328, 1991.
- [22] W. A. Tiller. *The Science of Crystallization*. Cambridge University Press, Cambridge, 1989.
- [23] A. Voigt and K.-H. Hoffmann. Control of Czochralski crystal growth. In *Optimal control of complex structures (Oberwolfach, 2000)*, volume 139 of *Internat. Ser. Numer. Math.*, pages 259–265. Birkhäuser, Basel, 2002.
- [24] J. S. Walker, D. Henry, and H. Ben Hadid. Magnetic stabilization of the buoyant convection in the liquid-encapsulated Czochralski process. *Journal of Crystal Growth*, 243:108–116, 2002.
- [25] L. M. Witkowski and J. S. Walker. Numerical solutions for the liquid-metal flow in a rotating cylinder with a weak transverse magnetic field,. *Fluid Dynamics Research*, 30:127–137, 2002.
- [26] L. M. Witkowski, J. S. Walker, and P. Marty. Nonaxisymmetric flow in a finite-length cylinder with a rotating magnetic field. *Physics of Fluids*, 11:1821–1826, 1999.